Journal of the Korean Astronomical Society
49: 199 ∼ 208, 2016 October

http://dx.doi.org/10.5303/JKAS.2016.49.5.199
pISSN: 1225-4614 · eISSN: 2288-890X
http://jkas.kas.org

Three-Site Photometric Monitoring of the δ Sct-Type Pulsating Star V1162 Orionis : Period Change and Its Implications for Pre-Main Sequence Evolution

Seung-Lee Kim[1,2], Sang-Mok Cha[1,3], Beomdu Lim[1], Jae Woo Lee[1,2], Chung-Uk Lee[1,2], Yongseok Lee[1,3], Dong-Jin Kim[1], Dong-Joo Lee[1], Jae-Rim Koo[1], Kyeongsoo Hong[1], Yoon-Hyun Ryu[1], and Byeong-Gon Park[1,2]

[1]Korea Astronomy and Space Science Institute, 776 Daedeokdae-ro, Yuseong-gu, Daejeon 34055, Korea; slkim@kasi.re.kr
[2]Korea University of Science and Technology, 217 Gajeong-ro, Yuseong-gu, Daejeon 34113, Korea
[3]School of Space Research, Kyung Hee University, 1732 Deogyeongdae-ro, Giheung-gu, Yongin, Kyeonggi 17104, Korea

Received September 9, 2016; accepted October 4, 2016

Abstract: We present photometric results of the δ Sct star V1162 Ori, which is extensively monitored for a total of 49 nights from mid-December 2014 to early-March 2015. The observations are made with three KMTNet (Korea Microlensing Telescope Network) 1.6 m telescopes installed in Chile, South Africa, and Australia. Multiple frequency analysis is applied to the data and resulted in clear detection of seven frequencies without an alias problem : five known frequencies and two new ones with small amplitudes of 1.2-1.7 mmag. The amplitudes of all but one frequency are significantly different from previous results, confirming the existence of long-term amplitude changes. We examine the variations in pulsation timings of V1162 Ori for about 30 years by using the times of maximum light obtained from our data and collected from the literatures. The $O-C$ (Observed minus Calculated) timing diagram shows a combination of a downward parabolic variation with a period decreasing rate of $(1/\mathrm{P})\mathrm{dP/dt} = -4.22 \times 10^{-6}$ year^{-1} and a cyclic change with a period of about 2780 days. The most probable explanation for this cyclic variation is the light-travel-time effect caused by an unknown binary companion, which has a minimum mass of 0.69 $\mathrm{M}_{\odot}$. V1162 Ori is the first δ Sct-type pulsating star of which the observed fast period decrease can be interpreted as an evolutionary effect of a pre-main sequence star, considering its membership of the Orion OB 1c association.

Key words: stars: variables: delta Scuti — stars: individual: V1162 Orionis — telescopes: KMTNet — techniques: photometric

1. Introduction

δ Sct-type pulsating stars are located in the lower portion of the Cepheid instability strip, on the main sequence with spectral types of A and F. Their pulsation periods are typically between 0.02 and 0.25 days which correspond to low-order pressure-modes (Breger 2000). Many of these stars show multiple periodicities with small amplitudes of less than 0.1 mag (Rodríguez & Breger 2001), pulsating in nonradial modes as well as radial ones. These observational features are very important because we can examine the stars' internal structure using asteroseismic techniques with multiple periods ; stellar interior is not accessible using the other methods. For this asteroseismic approach, some δ Sct stars were monitored for several years and/or observed extensively at multiple sites with different time zones, which resulted in successful detection of more than a few tens of pulsation frequencies ; for examples, 79 frequencies for FG Vir by Breger et al. (2005) and 64 frequencies for 4 CVn by Breger (2016).

The δ Sct stars with pulsation amplitude of $\Delta V \geq 0.30$ mag are called the HADS (high-amplitude δ Sct stars). It is generally accepted that the HADS are radial pulsators with slow rotation $v \sin i \leq 30$ km/sec (Breger 2000), although some of the stars may have additional nonradial modes with low amplitudes (McNamara 2000). Breger (2000) presented period changes of 18 radial mode δ Sct stars ; all but one star, IP Vir, are HADS. The observed rates of change in the periods were similar to but may not agree well with theoretical ones predicted using the evolution models of δ Sct stars. Models with convective core overshooting predict a large period change and fit the observed rate much better than those without the overshooting. Only the pre-main sequence stars are expected theoretically to have fast period decrease.

V1162 Ori ($V = 9.9$ mag, $B - V = 0.4$ mag) was discovered to be a δ Sct star by Lampens (1985), who estimated a period of 0.078686 days and full amplitude of 0.18 mag in the V-band. Poretti et al. (1990) suggested that this is a monoperiodic δ Sct star with a period of 0.07868614 days and amplitude of 0.22 mag in V. Several years later, Hintz et al. (1998) found that the amplitude decreased down to about 0.11 mag and the period increased noticeably to 0.07869165 days. The period and amplitude changes were investigated in more detail by Arentoft et al. (2001a,b) with extensive multisite campaign data. They detected eight frequencies and found cyclic variations with a period of about

Corresponding author: S.-L. Kim

280 days in the amplitude as well as the period.

V1162 Ori is often considered to be a HADS (Arentoft et al. 2001a), even though it has a smaller amplitude of about 0.1-0.2 mag and a higher rotational velocity of $v \sin i$ = 46.4 ± 4.0 km/sec (Solano & Fernley 1997) than the HADS. There may not be a strict discrimination between the HADS and the δ Sct stars with intermediate-amplitudes from 0.1 to 0.3 mag, in statistical distributions of the amplitude (Rodríguez & Breger 2001) and rotational velocity (Breger 2000). Solano & Fernley (1997) suggested that a value of ΔV = 0.1 mag is a better criterion to distinguish between high and low amplitude δ Sct stars. In this paper, we investigated the multi-periodicity and period variation of the δ Sct star V1162 Ori on the basis of new photometric data. The observation and data reduction are presented in Section 2. Multiple frequency analysis and pulsational characteristics are given in Section 3. We describe the pulsation timing variations in Section 4 and finally discuss our results in Section 5.

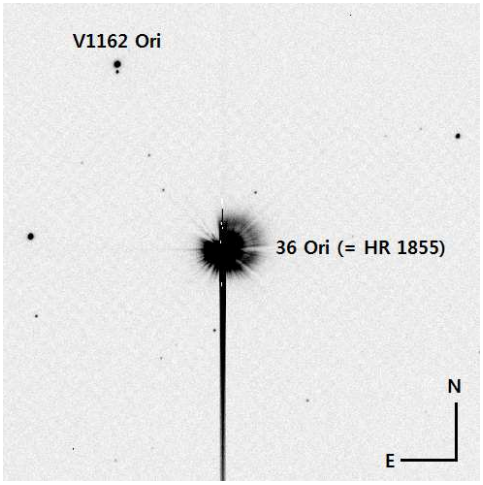

Figure 1. A zoomed sample image obtained with the KMTNet 18k mosaic CCD camera. The image size is about 7.0 × 7.0 square arcmin. Our target V1162 Ori is located at the north-east side of the very bright star 36 Ori. A faint close-by star with a separation of about 6.8 arcsec south from the target is clearly separated.

2. OBSERVATION AND DATA REDUCTION

2.1. Three-Site Monitoring

The observations of V1162 Ori were carried out for a total of 49 nights from December 2014 to March 2015, during the test run of three KMTNet 1.6 m telescopes. These telescopes, with a large FOV (field of view) of 2.0 by 2.0 square degrees, were installed at the CTIO (Cerro-Tololo Inter-American Observatory) in Chile, SAAO (South African Astronomical Observatory) in South Africa, and SSO (Siding Spring Observatory) in Australia. Imaging data were obtained with an 18k by 18k CCD camera, 2 by 2 mosaic of four 9k by 9k CCDs, at two sites of the KMTNet-CTIO and KMTNet-SAAO. We used a 4k CCD camera at the KMTNet-SSO site because the third 18k CCD camera was attached to the telescope on May 2015, two months after this observation period. All the raw CCD images were transferred from the three southern sites to the KMTNet data center in Korea via network communication and were preprocessed with the KMTNet pipeline. The KMTNet observation system and data handling process were described in more detail in our previous paper, Kim et al. (2016).

A finding chart for V1162 Ori is shown in Figure 1. The very bright star 36 Ori (= HR 1855, υ Ori; V = 4.63 mag) is located near the variable target. Although the bright star was strongly saturated and made a long streak in the CCD image, no interference with the variable star was observed. On the other hand, a faint close-by star, with a separation of about 6.8 arcsec south from the variable and with a brightness difference of about 3.4 mag in the B-band, could have influenced the variable star under bad seeing conditions. Fortunately, most of our data were obtained under good conditions of less than 2.0 arcsec and the effect from the close-by star was very limited. We applied aperture photometry to extract the instrumental magnitude of the stars, using the IRAF package. During this process the aperture radius was set at 3.2 arcsec to avoid any influence from this neighboring star.

We monitored V1162 Ori with only one filter in order to achieve high observational cadence, which is crucial for accurate multi-frequency analysis of short period δ Sct stars. The Johnson B filter was chosen because the target is so bright for our observation system that the exposure time necessary for the star to be unsaturated in the V-band was very short. Scintillation noise can be a dominant noise source when observing bright stars with short exposure times. For example, if the target is observed with an exposure time of 1.0 second and at an airmass of 1.4 (= zenith distance of about 45 degrees) in the KMTNet-SAAO site, the scintillation noise can be approximately estimated at 0.004 mag using Equation (1) of Gilliland & Brown (1992), which expresses the noise $\sigma_{scin} \propto {t_{exp}}^{-0.5}$. We also considered that the δ Sct-type stars have larger pulsation amplitudes in the B-band than in the V-band. Exposure time was set at 2 seconds for the 18k mosaic CCD camera and at 4 seconds for the 4k CCD camera, taking into account the difference of the quantum efficiency between the two detectors.

2.2. Ensemble Photometry

We applied the ensemble normalization technique (Kim et al. 1996) to standardize the instrumental magnitude of V1162 Ori, using eleven stars around the variable target. These stars have photometric parameters in a range of V = 9.79-14.24 and $(B-V)$ = 0.48-1.51, which values were extracted from the APASS (AAVSO Photometric All Sky Survey; Henden et al. 2016) catalogue. The transformation equation is,

$$B = b + a_1 + a_2 \times (B - V),$$

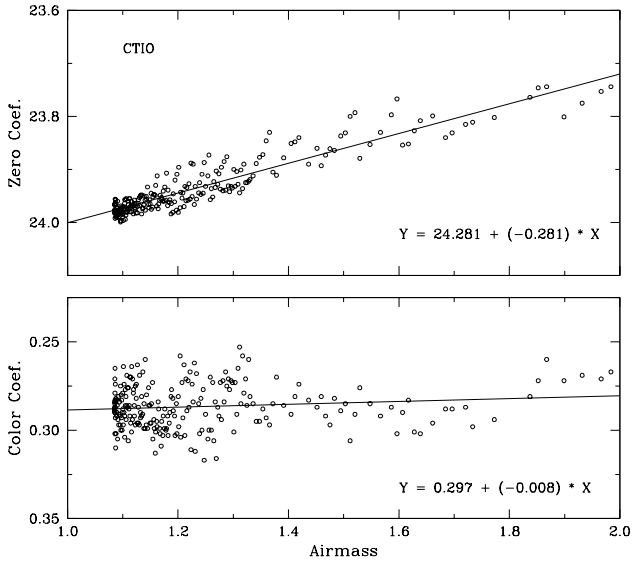

Figure 2. Variations of the transformation coefficients a_1 (photometric zero-point; upper) and a_2 (color dependent term; lower) along with the airmass. This is a sample result obtained from the KMTNet-CTIO data. The fitting values correspond to the instrumental zero magnitude, the first atmospheric extinction coefficient, the color transformation coefficient, and the second extinction coefficient, respectively, from the upper left.

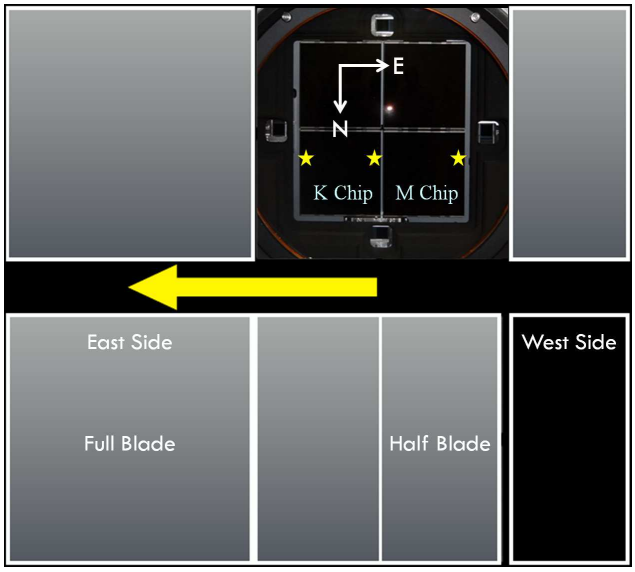

Figure 3. Schematic diagram of the opening (upper) and closing (lower) process of the KMTNet sliding shutter. The shutter consisted of one full blade for opening and two half blades for closing. There are four mosaic CCD chips for science imaging in the focal plane and another four small outside CCDs to guide the telescope. The optical orientation of the KMTNet system is reversed from the actual direction.

where B and b are the standard and instrumental magnitudes, respectively. The photometric zero-point (a_1) and color coefficient (a_2) were calculated for each time-series CCD image. We did not include the position dependency in the equation because the selected stars are within a field of 15 arcmin in diameter.

The coefficients a_1 and a_2 change linearly with the airmass, as shown in Figure 2, which is a sample result obtained from the KMTNet-CTIO data on December 19, 2014. These results imply that we can represent them using the following linear equations, $a_1 = a_{11} + a_{12} \times Airmass$ and $a_2 = a_{21} + a_{22} \times Airmass$. The $a_{11} = 24.281$ (± 0.009) and $a_{12} = -0.281$ (± 0.007) shown in the figure are equivalent to the instrumental zero magnitude and the first atmospheric extinction coefficient, respectively. The color dependent terms $a_{21} = 0.297$ (± 0.005) and $a_{22} = -0.008$ (± 0.004) correspond to the color transformation coefficient and the second extinction coefficient in order, for the KMTNet photometric system in the B-band.

2.3. Shutter Timing Correction

In the same way as other wide-field photometric survey systems like the PanSTARRS (Panoramic Survey Telescope And Rapid Response System; Kaiser et al. 2010), the KMTNet system adopted a large-format sliding shutter with rectangular blades of physical dimensions 310 mm by 310 mm. As shown in Figure 3, the full blade moves to the east upon receiving a signal from the camera controller to start the exposure and the two half blades move sequentially in the same direction when finishing the exposure. This kind of sliding shutter results in uniform illumination over the entire FOV, even with short exposure times of 1.0 second. On the other hand, the illuminating time is different across the focal plane, i.e., later at the east side than at the west. This timing lag could not be avoided due to a mechanical problem. Opposite to the physical direction, a star in the east field of the KMTNet CCD image starts (and stops) the exposure earlier than that in the west because the optical orientation of the KMTNet telescope is reversed at the focal plane.

In order to examine this timing lag, we observed the target V1162 Ori at three different positions of the 18k mosaic CCD image, i.e., the east edge in the so-called M chip (Figure 3), the west edge in the K chip, and near the center (the east edge of the K chip). The telescope pointing was changed from night to night in sequential order of the west-center-east positions. For the KMTNet-SSO site at which we used the 4k CCD camera and a self-contained small shutter with a negligible timing lag, the variable target was positioned all the time at the image center. The exposure start time in units of UT (Universal Time) was recorded at the CCD image header and converted to H.J.D. (Heliocentric Julian Date) at mid-exposure.

We derived the observation times at both maximum and minimum brightness of each pulsation cycle, and obtained the $O - C$ timing values using the same method as described in Section 4. The results are displayed in Figure 4, where we shifted the minimum timings to match with the maxima by using the averaged values of the two sets. The difference between the maximum timings and the minima deviated a little from

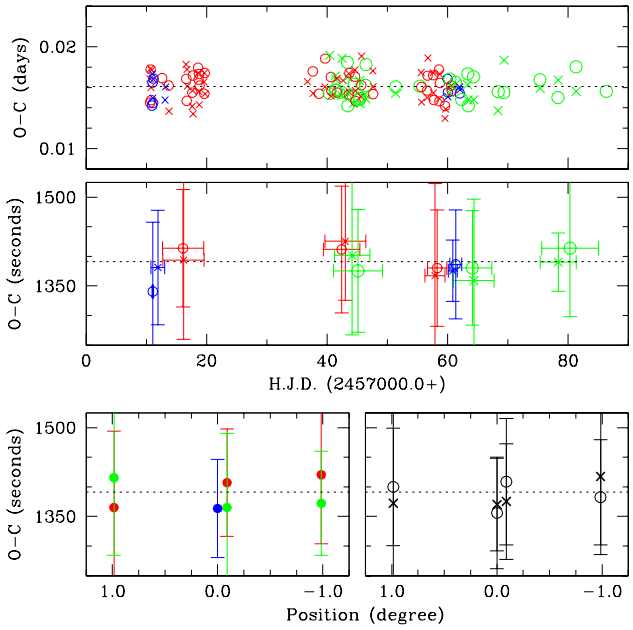

Figure 4. The $O-C$ values of the pulsation timings derived from our raw data. The data were divided into several sets to examine whether there was any systematic change along with the observation time (middle) and the east-to-west position (bottom). The 1σ value was calculated for each set and is displayed as an error bar. Red, green, and blue colors represent the data obtained at the KMTNet-CTIO, KMTNet-SAAO, and KMTNet-SSO sites, respectively. The open circles are the maximum timings and the crosses are the minima.

0.5 times the pulsation period because V1162 Ori has asymmetric light curves that show faster brightening than darkening (see Figure 5); this is the same shape as the usual HADS (McNamara 2000).

The $O-C$ values were nearly constant during our observing span of about 70 days, as shown in Figure 4. We divided the full data into several sets to examine whether there was any systematic change along with the observation time and the east-to-west position. The error bars in the figure are root-mean-square errors (1σ) for each data set. Unfortunately, we could not detect the systematic difference in timings between the east field (position of +1.0 degree) and the west field observations. The trends were not consistent between the two sites of KMTNet-CTIO and KMTNet-SAAO (bottom left figure). The maxima and minima (bottom right one) were also inconsistent. In fact, the pulsation timings turned out to have large uncertainties of several tens of seconds, compared with the shutter moving time of a few seconds. The large error may primarily be caused by the long observational cadence due to the long overhead time of more than 70 seconds for the 18k CCD camera (Kim et al. 2016).

Although we failed to determine the shutter timing lag from the above $O-C$ analysis, we corrected the timing lag by using the blade moving time which was measured to be about 5.1 seconds. Considering the difference in the physical size between the shutter blade and the mosaic CCD chips, the east edge of the CCD starts to receive photons about 1.0 second later than the open time of the full blade (i.e., the exposure start time recorded in the image header) and the west edge receives photons about 4.1 seconds later. Such a systematic timing deviation may not be ignorable in some research fields required high timing accuracy of less than ~10 seconds; for example, in the detection of exoplanets using the timing method (Silvotti et al. 2007; Lee et al. 2009) and observation of the terrestrial parallax in a microlensing event (Gould et al. 2009).

Light variations of V1162 Ori after correcting the shutter timing lag are displayed in Figure 5, in which the red points represent the data obtained from the KMTNet-CTIO site, the green from the KMTNet-SAAO, and the blue from the KMTNet-SSO. The solid lines are synthetic curves obtained from the multiple-frequency analysis described in the following section. Typical error of the data was about 0.007 mag, estimated from root-mean-square errors of the non-variable stars used for the ensemble photometry.

3. PULSATIONAL CHARACTERISTICS

The light variations of V1162 Ori changed its shape from cycle to cycle, as shown in Figure 5. This feature is found in most δ Sct-type pulsating stars and implies that multiple periods are superimposed in the observed variations. In order to investigate the multiple periodicity of V1162 Ori, we applied the discrete Fourier transform and the nonlinear least square fitting method (Kim et al. 2010) to the data. Results from this multi-frequency analysis are listed in Table 1 and displayed in Figure 6. The errors in frequency, amplitude, and phase were calculated from the equations by Montgomery & O'Donoghue (1999). The figure shows very low amplitudes at the 1.0 c/d (cycles day^{-1}) alias frequency multiplets, estimated to be $\leq$40% of the signal frequency. This is nearly half the amplitude level obtained from the single site data (Breger 2000). The photometric monitoring at the three KMTNet sites with different time zones, therefore, gives us a very important advantage in our attempt to reduce the contamination from the alias frequencies. We detected a total of seven frequencies resulting from the successive and simultaneous prewhitening process, with a criterion of S/N (signal to noise amplitude ratio) higher than 4.0, following Breger et al. (1993).

Arentoft et al. (2001a) detected eight frequencies in their multisite campaign data. The primary frequency f_1 and its two harmonics $2f_1$ and $3f_1$ are nearly the same as ours. And their f_3 = 19.1701 c/d is well matched with our f_3 = 19.16927 c/d. Arentoft et al. (2001a) noted that their f_5 = 15.9901 c/d may have suffered from the 1.0 c/d aliasing problem. Arentoft et al. (2001b) confirmed this aliasing feature. Our f_5 = 16.98823 c/d is a true frequency, corresponding to their f_5. We could not detect the other three frequencies of 12.9412 c/d, 21.7186 c/d, and 27.7744 c/d, of which the amplitudes decreased to less than about 1.5 mmag during our observing runs, as shown in Figure 6. Arentoft

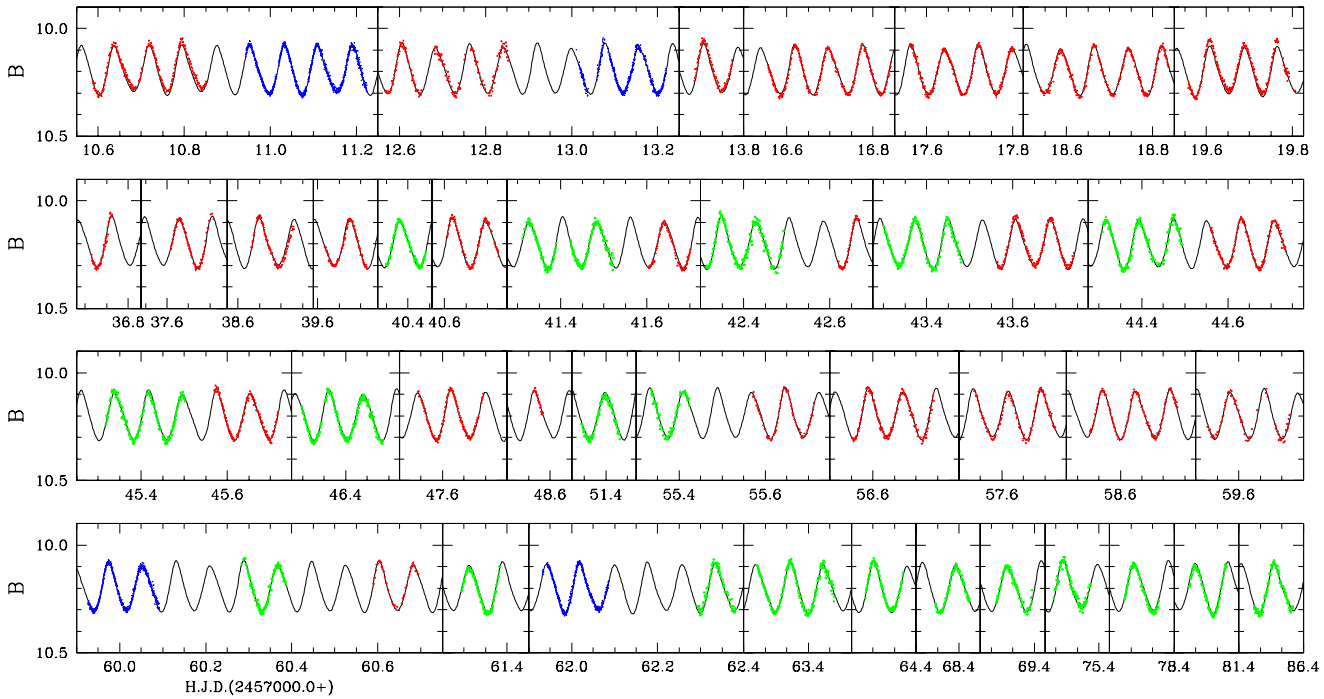

Figure 5. Light variations of the δ Sct star V1162 Ori. The colored points are the observed data obtained at the three KMTNet sites for a total 49 nights from December 2014 to March 2015. The colors are the same as in Figure 4. The lines are synthetic curves calculated using multiple-frequency analysis.

Table 1
Results of the multiple frequency analysis of V1162 Ori.

Frequency† (c/d)	Ampl.† (mag)	Phase† (rad)	S/N‡	Remark
$f_1 = 12.70896$	0.1074	1.673	219.3	F-mode
± 0.00001	± 0.0002	± 0.002	–	
$f_2 = 25.41801$	0.0126	1.16	37.0	$2f_1$
± 0.00010	± 0.0002	± 0.01	–	
$f_3 = 19.16927$	0.0094	4.97	23.0	nonradial
± 0.00014	± 0.0002	± 0.02	–	
$f_4 = 38.12584$	0.0036	6.10	12.8	$3f_1$
± 0.00036	± 0.0002	± 0.05	–	
$f_5 = 16.98823$	0.0019	1.13	4.3	nonradial
± 0.00070	± 0.0002	± 0.09	–	
$f_6 = 31.87708$	0.0017	4.09	6.1	$f_1 + f_3$
± 0.00082	± 0.0002	± 0.10	–	
$f_7 = 50.83633$	0.0012	5.22	5.1	$4f_1$
± 0.00105	± 0.0002	± 0.14	–	

†Frequencies (f_j), amplitudes (A_j), and phases (ϕ_j) are values of the equation $m = m_0 + \Sigma_j A_j cos\{2\pi f_j(t - t_0) + \phi_j\}$, t_0 = H.J.D. 2457000.
‡Noise values of the S/N were calculated from averaging the residual amplitudes in a range of ± 5 c/d for each frequency.

et al. (2001b) had already found that the amplitude of their $f_2 = 12.9412$ c/d decreased continuously from about 4.5 mmag around H.J.D. 2450850 to 0.7 mmag around H.J.D. 2451950. They also showed that the amplitudes of their $f_4 = 21.7186$ c/d and $f_6 = 27.7744$ c/d decreased to about 1.3 mmag and 0.6 mmag, being about half the amplitudes of 2.4 mmag and 1.1 mmag, respectively, obtained in their former study (Arentoft et al. 2001a). Therefore, the amplitude decrease of these three frequencies, and then our failure to detect them, would not be a surprising thing. On the contrary, we detected two new frequencies of $f_6 = 31.87708$ c/d with an amplitude of 1.7 mmag and $f_7 = 50.83633$ c/d with an amplitude of 1.2 mmag. The former turned out to be a combination frequency of $f_1 + f_3$ and the latter to be a harmonic frequency of $4f_1$. There remain two peaks in the frequency range higher than 4.0 c/d, in which pressure mode oscillations of δ Sct-type stars are detected (Breger 2000). The frequency of 6.461 c/d with an amplitude of about 2.3 mmag seems to be a combination frequency of $f_3 - f_1$, although its S/N is lower than the criterion of 4.0 due to the rather high amplitude noise in this low frequency region. Another peak at 8.661 c/d may be its aliasing frequency.

The dominant frequency f_1 was also found to experience amplitude change over time, being 92 mmag at H.J.D. 2445738-6043 (Lampens 1985), 98 mmag at H.J.D. 2447108-208 (Poretti et al. 1990), 72 mmag at H.J.D. 2449992-50407, 50 mmag around H.J.D. 2450465 (Hintz et al. 1998), and 66.6 mmag at H.J.D. 2450818-1662 (Arentoft et al. 2001a). The amplitude of f_1 increased noticeably in our data to be 107.4 mmag in the B-band, which is equivalent to 82.6 mmag in the V-band, applying the amplitude difference of V1162 Ori between two passbands, $\Delta B/\Delta V = 1.3$, obtained empirically from the data by Poretti et al. (1990). The amplitude of $f_3 = 19.16927$ c/d was 9.4 mmag in our B-band data, corresponding to 7.2 mmag in the V-band. This is more than two times the previous value

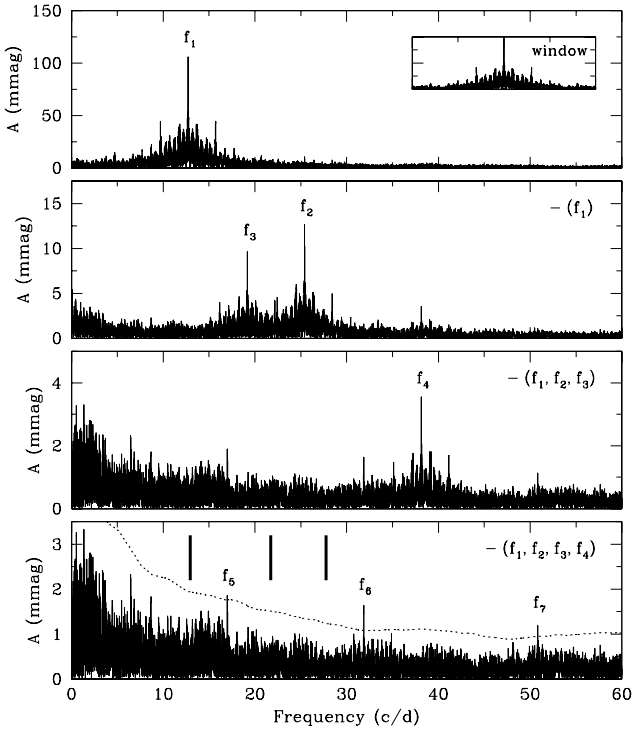

Figure 6. Amplitude spectra of V1162 Ori. The window spectrum is displayed in the right corner of the top panel. We detected seven frequencies resulting from the successive prewhitening process. The dashed line at the bottom corresponds to four times the noises that were calculated from averaging the residual amplitudes after subtracting all seven frequencies. Thick vertical bars indicate the locations of the three frequencies discovered previously by Arentoft et al. (2001a) but undetected in our data.

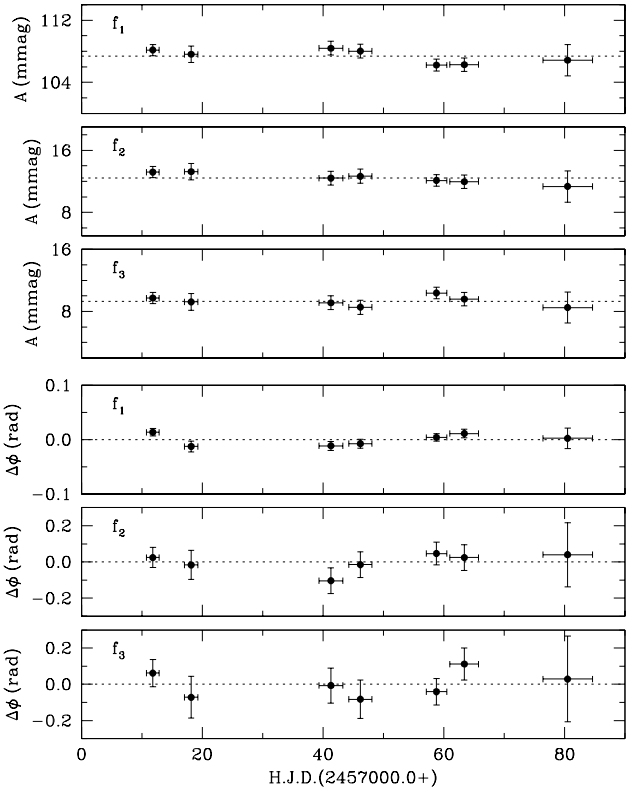

Figure 7. Amplitude (upper) and phase (lower) variations of three high amplitude frequencies f_1, f_2, and f_3. Following Arentoft et al. (2001a), the vertical error bars are displayed to be twice the formal errors by Montgomery & O'Donoghue (1999).

obtained by Arentoft et al. (2001a,b). The amplitude of $f_5 = 16.98823$ c/d, 1.9 mmag in B or 1.5 mmag in V, was similar to the pervious result of about 1.6 mmag obtained by Arentoft et al. (2001b). The amplitude increases of our f_1 and f_3 could have resulted in the new detection of their combination frequencies ($f_1 + f_3$ and probably $f_3 - f_1$) and the high-order harmonic $4f_1$.

Arentoft et al. (2001a) obtained a very interesting result from their data that both the amplitude and the phase of the frequency f_1 changed cyclically with a period of 282 days. During this cycle period, the phase variations appeared to be shifted nearly a quarter from the amplitude variations. These variations could be interpreted as the modulation of two very closely-separated frequencies; the researchers found a residual signal at 12.71197 c/d with 13 mmag, near f_1 (= 12.708264 c/d). In order to check these changes in our data, we examined the amplitude and the phase (A, ϕ) variations of the three high amplitude frequencies, f_1, f_2, and f_3, using the same procedure as they used. At first, we subtracted the synthetic curves of the six frequencies f_2-f_7 from the original data and obtained light variations of only f_1. Then, the data were divided into seven sets with a time span of about 5-10 days. We fitted sinusoidal curves of f_1 to each data set and obtained the amplitudes and phases of f_1. The same procedure was applied to the other two frequencies f_2 and f_3. As can be seen in Figure 7, the amplitudes and phases of all three frequencies turned out to be nearly constant during our observing runs. Considering the timing shift between the amplitude and the phase variations shown in the previous data, the constancy in our data may not be caused by the short time span of about 70 days. This implies that our data did not experience the modulation phenomenon of two close frequencies, which is different from the previous results.

We calculated the observed pulsation constant of f_1 using the equation $\log Q_1 = -\log f_1 + 0.5 \log g + 0.1 M_{bol} + \log T_{\rm eff} - 6.456$ (Breger 2000), where the frequency f_1 is in units of c/d. The physical properties of V1162 Ori were adopted from the results of the $uvbyH_\beta$ photometry by Hintz et al. (1998): surface gravity $\log g$ = 3.96, absolute bolometric magnitude $M_{bol} = 2.0$, and effective temperature $T_{\rm eff} = 7540$ K. The resulting value $Q_1 = 0.0314 \pm 0.0025$ is in good agreement with the theoretical value of 0.0327-0.0331 (Breger 1979; Fitch 1981) for the radial fundamental mode (i.e. F-mode); the primary error source in Q came from the surface gravity of $\sigma(\log g) = 0.07$. The f_1's peak-to-valley amplitude ΔB of about 0.2 mag would be too high to be interpreted as the nonradial mode. The absolute V magnitude $M_v = 2.1$ estimated from the $uvbyH_\beta$

Table 2
Pulsation Maximum Timings of V1162 Ori.

T_{max}†	Cycles	$O-C$	T_{max}†	Cycles	$O-C$	T_{max}†	Cycles	$O-C$	T_{max}†	Cycles	$O-C$
10.6370	125812	−0.0017	19.6886	125927	+0.0013	44.7075	126245	−0.0012	59.9747	126439	+0.0014
10.7192	125813	+0.0018	37.6288	126155	+0.0016	45.3371	126253	−0.0011	60.0520	126440	+0.0000
10.7946	125814	−0.0015	38.6493	126168	−0.0008	45.4161	126254	−0.0007	60.3679	126444	+0.0012
10.9514	125816	−0.0020	39.6764	126181	+0.0035	45.6533	126257	+0.0004	60.6034	126447	+0.0006
11.0324	125817	+0.0003	40.3806	126190	−0.0005	46.3615	126266	+0.0005	60.6825	126448	+0.0011
11.1096	125818	−0.0012	40.6183	126193	+0.0011	46.4421	126267	+0.0024	61.3118	126456	+0.0009
11.1905	125819	+0.0010	40.6956	126194	−0.0002	47.6196	126282	−0.0004	62.0180	126465	−0.0011
12.6065	125837	+0.0007	41.3252	126202	−0.0001	51.3974	126330	+0.0006	62.3331	126469	−0.0007
13.7074	125851	+0.0000	41.4826	126204	−0.0001	55.4101	126381	+0.0004	63.3584	126482	+0.0017
16.6197	125888	+0.0011	41.6397	126206	−0.0003	55.6463	126384	+0.0006	63.4343	126483	−0.0011
16.6963	125889	−0.0010	42.3479	126215	−0.0003	56.5899	126396	−0.0000	64.3024	126494	+0.0015
17.6409	125901	−0.0006	43.3737	126228	+0.0026	56.6701	126397	+0.0015	68.3933	126546	+0.0009
17.7212	125902	+0.0010	43.4481	126229	−0.0017	57.6144	126409	+0.0016	69.3367	126558	+0.0001
18.5875	125913	+0.0018	43.6070	126231	−0.0001	57.6906	126410	−0.0009	75.3180	126634	+0.0014
18.6644	125914	−0.0000	43.6874	126232	+0.0016	58.5591	126421	+0.0021	78.3062	126672	−0.0003
18.7443	125915	+0.0012	44.3932	126241	−0.0008	58.6347	126422	−0.0010	81.2993	126710	+0.0028
18.8218	125916	+0.0000	44.4731	126242	+0.0005	58.7152	126423	+0.0008	86.3327	126774	+0.0005
19.6079	125926	−0.0007	44.6312	126244	+0.0012	59.5790	126434	−0.0009			

†Observed maximum times (H.J.D. +2457000.0).

photometry is nearly the same as the value of $M_v = 2.14$ derived from the period-luminosity relation of the HADS, $M_v = -3.725 \log P_0 - 1.969$ (McNamara 2000), where P_0 is a period of the radial fundamental mode in the unit of days. Consequentially, we identified the primary frequency f_1 of V1162 Ori as the radial fundamental mode. The other two pulsating frequencies of $f_3 = 19.16927$ c/d and $f_5 = 16.98823$ c/d have period ratios of $f_1/f_3 = 0.663$ and $f_1/f_5 = 0.748$. These observed ratios could not be matched with the theoretical values between the two radial modes, $P_1/P_0 = 0.761$ for the first overtone mode (P_1) and $P_2/P_0 = 0.616$ for the second overtone (P_2). This indicates that the two frequencies with small amplitudes were excited in nonradial modes; the period ratio is a good indicator that can be used to discriminate between the radial and nonradial modes because the value can be determined very precisely and may be much less dependent on theoretical models than the pulsation constant Q.

4. PULSATION TIMING VARIATION

Long-term variations of the timings of pulsation maxima were reported in previous studies by Hintz et al. (1998), Arentoft & Sterken (2000), and Arentoft et al. (2001a,b). The latest results showed that the variations can be interpreted as a combination of the secular period decrease with $(1/\mathrm{P})\mathrm{dP/dt} = -1.6 \times 10^{-5}$ year^{-1} and cyclic change with a period of 277 days (Arentoft et al. 2001b). In order to investigate these variations on the basis of the longer time span, including the recent new data, we determined the times of maximum brightness of each pulsation cycle by fitting third degree polynomials to the data. A total of 71 maximum times were obtained from our data and are listed in Table 2. Typical measurement error in the individual timing was about 0.0005 days. Additional 433 pulsation maxima were collected from the literatures (Hintz et al. 1998; Arentoft & Sterken 2000; Arentoft et al. 2001a,b; Khokhuntod et al. 2011; Wils et al. 2010, 2011, 2012, 2013, 2014, 2015). The $O-C$ diagrams of all maximum times are displayed in Figure 8.

Initially, we obtained the calculated values from the equation $C = T_0 + P \times E$, for which we adopted the previous maximum epoch of T_0 = H.J.D. 2447110.7776 by Poretti et al. (1990) and the period of $P = 0.07868910$ days by Arentoft et al. (2001a). The cycle count E is the integer value of $(O-T_0)/P$ and its decimal number corresponds to the $O-C$ value. If the maximum timings change larger than one periodic cycle, the $O-C$ values appear to have jumped up or down by the amount of one cycle, as shown by Khokhuntod et al. (2011). After testing several cases, therefore, we corrected the cycle counts to ensure continuity of the variation trend and to minimize the fitting residuals. The resulting diagram shows well-defined continuous variations for the whole set of data with a long time span of about 30 years. The corrected cycle counts of our data are listed as Cycles in Table 2.

Following the previous studies by Arentoft et al. (2001a,b), we fitted a parabolic function first and found a cyclic change from the residuals. Next, both the parabolic and cyclic functions were simultaneously fitted to the data, as follows:

$$\begin{aligned} C_{full} &= T_0 + P\,E + A\,E^2 + \tau_2 \\ &= 2447110.7004(11) + \\ &\quad 0.07869278(3)E - 3.58(2) \times 10^{-11} E^2 + \\ &\quad 0.0084(3)\sin(0.0001780(7)E + 4.37(3)) \end{aligned}$$

where the numbers in parentheses are 1σ values for the last digit of each term. The cyclic variation τ_2 is dis-

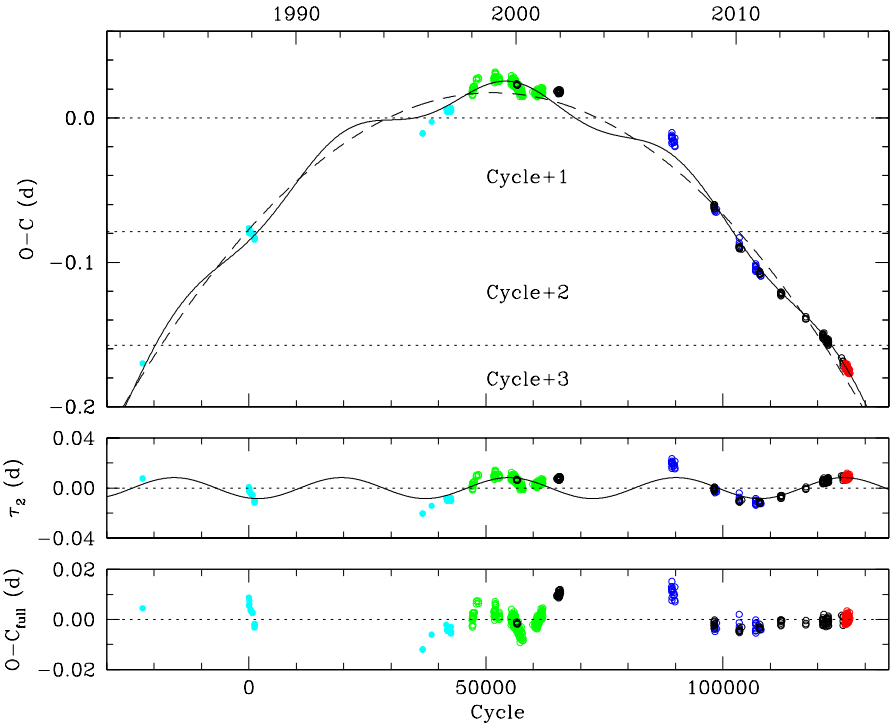

Figure 8. The $O-C$ diagrams of the pulsation maximum timings. Some $O-C$ data appeared to have overflowed outside one pulsation cycle and then their cycle counts were corrected to ensure continuity of the variation trend. Colors represent the different data sources : cyan for data collected by Hintz et al. (1998), green by Arentoft & Sterken (2000) and Arentoft et al. (2001a,b), blue by Khokhuntod et al. (2011), black by Wils et al. (2010, 2011, 2012, 2013, 2014, 2015), and red for our data.

played in the middle of Figure 8. The $O-C_{full}$ values of our data are given as $O-C$ in Table 2. Their residual scatter was estimated to be 0.0011 days.

The downward parabola indicates the period decrease. The value of $A = 0.5\,\mathrm{P}\,\mathrm{dP/dt} = -3.58 \times 10^{-11}$ days can be converted to the period change rate of $(1/\mathrm{P})\mathrm{dP/dt} = -4.22\ (\pm 0.03) \times 10^{-6}$ year^{-1}, as presented by Breger & Pamyatnykh (1998). This decreasing rate is one order of magnitude smaller than the previous result of -1.6×10^{-5} year^{-1} obtained by Arentoft et al. (2001b), who analyzed the data with the time span of about 15 years, half the span of our analysis. In spite of that, our new value is still two orders of magnitude larger than the theoretical result of about 10^{-8} year^{-1} for normal δ Sct-type main sequence stars (Breger & Pamyatnykh 1998). Furthermore, pulsation periods of normal δ Sct stars would be expected to increase because main sequence stars grow larger during most of their evolution time up to the giant phase. Therefore, the rapid period decrease of V1162 Ori could not be explained by the evolution effect of normal δ Sct stars.

As shown in Figure 1, V1162 Ori is located very closely to the bright star υ Ori (= 36 Ori) with the spectral type O9.7V (Sota et al. 2011), which is known to be one of the massive stars in the Orion OB 1c association (Smith 1981; Nieva & Przybilla 2012). We estimated the distance of V1162 Ori to be about 360 ± 30 pc from the parameters of $V = 9.89$ mag, $\mathrm{E}(b-y) = 0.021$, and $M_v = 2.1$ mag (Arentoft & Sterken 2000). The star's parallax of 2.59 ± 0.28 mas (milli-arcsec), released very recently by *Gaia* project (2016), can be converted to the distance of 386^{+38}_{-47} pc. These values are in good agreement with the distance of about 400 pc for the Orion OB 1c association with the very young age of 2-6 Myr (Bally 2008) and is nearly the same as the spectroscopic distance 366 ± 24 pc of 36 Ori (Nieva & Przybilla 2012). This means that V1162 Ori is not a main sequence star but a pre-main sequence star as a member of the Orion OB 1c association. Evolution models of pre-main sequence stars by Siess et al. (2000) give us a hint that V1162 Ori has an age of about 10 Myr and is in the contracting phase, having still not arrived at the zero-age main sequence. This age is very different from the previous value of 0.6 Gyr (Hintz et al. 1998), which was derived from the evolutionary models of main sequence stars.

Breger & Pamyatnykh (1998) presented theoretical period changes of δ Sct stars in the $\log g$ versus $\log T_{eff}$ diagram. According to their results, the pre-main sequence star V1162 Ori is expected to have a period changing rate of about -5×10^{-7} year^{-1}. They also showed that, for main sequence stars, evolution models with convective core overshooting predict larger period changing rates than those without the overshooting. Therefore, we believe that the observed period decrease of V1162 Ori can be explained as the evolution effect of a pre-main sequence star, although the observed rate is

one order of magnitude larger than the theoretical one. More realistic theoretical models considering the overshooting effect for pre-main sequence stars (Marques et al. 2006) may remove the present conflict between the observed and theoretical period changing rates.

In addition to the dominant parabolic change, we found a cyclic variation with a frequency of 0.0000283 ($= 0.0001780/2\pi$) cycle^{-1} and an amplitude of 0.0084 days. The frequency can be converted to a period of about 2780 days ($\approx$ 7.6 years). Our results were very different from the previous ones by Arentoft et al. (2001a,b) showing a period of about 280 days. They suggested two possible explanations for the short-term cyclic variation. One is the light-travel-time effect caused by the motion of the pulsating star in a binary system and the other is the beating phenomenon of two (or more) very closely-separated frequencies. As shown in the bottom of Figure 8, the short-term variation disappeared in the recent data from the year 2009. These significant deviations from regularity clearly rule out the binary hypothesis as an explanation of the cyclic variation. The beating may be the only remaining explanation for the previous short-term variation.

The new cyclic variation with a period of about 2780 days may not be correlated with the amplitude change of f_1, differing from the short-term variation (see Section 3). This implies that the long-term cyclic variation did not result from the beating phenomenon of two frequencies. Therefore, the most probable hypothesis is the light-travel-time effect caused by the unknown companion. If we accept this hypothesis and adopt the evolutionary mass of 1.8 $M_\odot$ obtained by Hintz et al. (1998), V1162 Ori has a binary companion with a mass of $m \sin i = 0.69$ $M_\odot$ and with the distance of $a \sin i = 1.4$ AU from the pulsating primary star, assuming a circular orbit with an inclination angle of i.

5. CONCLUSIONS

We carried out photometric monitoring of the δ Sct star V1162 Ori to investigate its multi-periodicity and period variation. Our data were obtained for a total of 49 nights from December 2014 to March 2015. The observations were made at the three KMTNet sites, which are spread over different southern continents and are located at similar latitudes of about -30 degrees. This telescope network enables us to monitor a target continuously for 24 hours without stopping in the daytime. As a result, we found seven frequencies from the multiple frequency analysis, with considerably low contamination of their alias frequencies, as shown in Figure 6 : five known frequencies from the previous multisite campaign by Arentoft et al. (2001a) and two new ones with small amplitudes of 1.2-1.7 mmag. The amplitudes of all frequencies but our f_5 were significantly different from the previous results, confirming that the amplitude changes with time. These results illustrate the outstanding capability of the KMTNet system in the photometric monitoring of variable objects.

By using the pulsation maximum times obtained from our data and collected from the literatures, we examined the timing variations of V1162 Ori for about 30 years. The $O - C$ diagram showed a combination of downward parabolic variation with a period decreasing rate of $(1/\mathrm{P})\mathrm{dP/dt} = -4.22 \times 10^{-6}$ year^{-1} and a cyclic change with a period of about 2780 days and an amplitude of 0.0084 days. The most probable explanation on this cyclic variation is the light-travel-time effect caused by an unknown binary companion with a minimum mass of 0.69 $M_\odot$.

The observed period decreasing of V1162 Ori differs greatly from the theoretical expectation of normal δ Sct-type main sequence stars. Breger & Pamyatnykh (1998) predicted theoretically that only pre-main sequence stars have a period decreasing rate faster than $(1/\mathrm{P})\mathrm{dP/dt} = -1.0 \times 10^{-7}$ year^{-1}. We found that V1162 Ori is a pre-main sequence star as a member of the Orion OB 1c association and this is the first δ Sct-type star of which the observed period change can be interpreted as an evolutionary effect of a pre-main sequence star. Due to the short life-time in the δ Sct instability strip, the pre-main sequence δ Sct-type stars have a much smaller population than the main sequence stars. There were only eight pre-main sequence stars among a total of 636 δ Sct stars discovered up to January 2000 (Rodríguez & Breger 2001). All of these pre-main sequence stars have low amplitudes of less than $\Delta V = 0.04$ mag. In conclusion, V1162 Ori is the best target to test the evolution models of pre-main sequence stars with intermediate mass of about 2.0 $M_\odot$ using the period decreasing rate.

ACKNOWLEDGMENTS

We are very grateful to Prof. Hwankyung Sung for his valuable comments. We thank Mr. Seung-Won Ko and Min-Jun Kim for their help in obtaining the data at the KMTNet-CTIO site. This work was supported by KASI grant 2016-1-832-01. One of the authors, K. Hong, was supported by Basic Science Research Program through the National Research Foundation of Korea (NRF) funded by the Ministry of Education (grant number: NRF-2016R1A6A3A01007139). This research has made use of the KMTNet system operated by KASI and the data were obtained at three host sites of CTIO in Chile, SAAO in South Africa, and SSO in Australia.

REFERENCES

Arentoft, A., & Sterken, C. 2000, Period and Amplitude Changes in the δ Scuti Star V 1162 Orionis, A&A, 354, 589

Arentoft, A., Sterken, C., Handler, G., et al. 2001a, V1162 Ori: A Multiperiodic δ Scuti Star with Variable Period and Amplitude, A&A, 374, 1056

Arentoft, A., Sterken, C., Knudsen, M. R., et al. 2001b, Irregular Amplitude Variations and Another Abrupt Period Change in the δ Scuti Star V1162 Ori, A&A, 378, L33

Bally, J. 2008, Overview of the Orion Complex, in Handbook of Star Forming Regions Vol. I: The Northern Sky, ed. B. Reipurth, ASP Monograph Publications, 4, 459

Breger, M. 1979, Delta Scuti and Related Stars, PASP, 91, 5

Breger, M. 2000, δ Scuti Stars (Review), in Delta Scuti and Related Stars, ed. M. Breger, & M. H. Montgomery, ASP Conference Series, 210, 3

Breger, M. 2016, Nonradial and Radial Period Changes in the δ Scuti Star 4 CVn I. 700+ Nights of Photometry, A&A, 592, A97

Breger, M., & Pamyatnykh, A. A. 1998, Period Changes of δ Scuti Stars and Stellar Evolution, A&A, 332, 958

Breger, M., Stich, J., Garrido, R., et al. 1993, Nonradial Pulsation of the Delta Scuti Star BU Cancri in the Praesepe Cluster, A&A, 271, 482

Breger, M., Lenz, P., Antoci, V., et al. 2005, Detection of 75+ Pulsation Frequencies in the δ Scuti Star FG Virginis, A&A, 435, 955

Fitch, W. S. 1981, $\ell = 0$, 1, 2, and 3 Pulsation Constants for Evolutionary Models of δ Scuti Stars, ApJ, 249, 218

Gaia Collaboration, 2016, VizieR Online Data Catalogue : *Gaia* DR1

Gilliland, R. L., & Brown, T. M. 1992, Limits to CCD Ensemble Photometry Precision and Prospects for Asteroseismology, PASP, 104, 582

Gould, A., Udalski, A., Monard, B., et al. 2009, The Extreme Microlensing Event OGLE-2007-BLG-224: Terrestrial Parallax Observation of a Thick-Disk Brown Dwarf, ApJ, 698, L147

Henden, A. A., Templeton, M., Terrell, D., Smith, T. C., Levine, S., & Welch, D. 2016, AAVSO Photometric All Sky Survey (APASS), DR9

Hintz, E. G., Joner, M. D., & Kim, C. 1998, Photometric Studies of δ Scuti Stars. II. V1162 Orionis, PASP, 110, 689

Kaiser, N., Burgett, W., Chambers, K., et al. 2010, The Pan-STARRS Wide-Field Optical/NIR Imaging Survey, Proceeding of SPIE, 7733-0E

Khokhuntod, P., Zhou, A.-Y., Boonyarak, C., & Jiang, S.-Y. 2011, V1162 Orion: Updated Amplitude and Period Variation, IBVS (arXiv:1109.3840)

Kim, S.-L., Chun, M.-Y., Park, B.-G., & Lee, S.-W. 1996, Variable Stars in a Field of the Old Open Cluster M67 : Photometric Precision of the BOAO 1.8 m Telescope, JKAS, 29, 43

Kim, S.-L., Lee, J. W., Lee, C.-U., & Youn, J.-H. 2010, Algol-Type Eclipsing Binaries with δ Scuti-Type Pulsating Components: IV Cas, PASP, 122, 1311

Kim, S.-L., Lee, C.-U., Park, B.-G., et al. 2016, KMTNet: A Network of 1.6 m Wide-Field Optical Telescopes Installed at Three Southern Observatories, JKAS, 49, 37

Lampens, P. 1985, BD-7°1108, A New Delta Scuti Variable, IBVS, no. 2794

Lee, J. W., Kim, S.-L., Kim, C.-H., Koch, R. H., Lee, C.-U., Kim, H.-I., & Park, J.-H. 2009, The sdB+M Eclipsing System HW Virginis and Its Circumbinary Planets, AJ, 137, 3181

Marques, J. P., Monteiro, M. J. P. F. G., & Fernandes, J. 2006, On the Effect of Overshooting as Predicted by the Modelling of the Pre-main-Sequence Evolution of a $2M_\odot$ Star, MNRAS, 371, 293

McNamara, D. H. 2000, The High-Amplitude δ Scuti Stars, in Delta Scuti and Related Stars, ed. M. Breger, & M. H. Montgomery, ASP Conference Series, 210, 373

Montgomery, M. H., & O'Donoghue, D. 1999, A Deviation of the Errors for Least Square Fitting to Time Series Data, DSSN, 13, 28

Nieva, M.-F., & Przybilla, N. 2012, Present-Day Cosmic Abundances. A Comprehensive Study of Nearby Early B-type Stars and Implications for Stellar and Galactic Evolution and Interstellar Dust Models, A&A, 539, A143

Poretti, E., Antonello, E., & Le Borgne, J. F. 1990, Fourier Decomposition of the Light Curves of Pulsating Variables: The Delta Scuti stars BD-7°1108, KU Centauri and V567 Ophiuchi, A&A, 228, 350

Rodríguez, E., & Breger, M. 2001, δ Scuti and Related Stars: Analysis of the R00 Catalogue, A&A, 366, 178

Siess, L., Dufour, E., & Forestini, M. 2000, An Internet Server for Pre-Main Sequence Tracks of Low- and Intermediate-Mass Stars, A&A, 366, 178

Silvotti, R., Schuh, S., Janulis, R., et al. 2007, A Giant Planet Orbiting the Extreme Horizontal Branch Star V 391 Pegasi, Nature, 449, 189

Smith, M. A. 1981, Nonradial Pulsations in the Zero-Age Main-Sequence Star Upsilon Orionis (09.5 V), ApJ, 248, 214

Solano, E., & Fernley, J. 1997, Spectroscopic Survey of δ Scuti Stars I. Rotation Velocities and Effective Temperatures, A&AS, 122, 131

Sota, A., Maíz, A. J., Walborn, N. R., et al. 2011, The Galactic O-Star Spectroscopic Survey. I. Classification System and Bright Northern Stars in the Blue-Violet at R $\sim$ 2500, ApJS, 193, 24

Wils, P., Hambsch, F.-J., Lampens, P., et al. 2010, Maxima of High-Amplitude Delta Scuti Stars, IBVS, no. 5928

Wils, P., Hambsch, F.-J., Robertson, C. W., et al. 2011, Maxima of High-Amplitude Delta Scuti Stars, IBVS, no. 5977

Wils, P., Panagiotopoulos, K., Van Wassenhove, J., et al. 2012, Photometry of High-Amplitude Delta Scuti Stars, IBVS, no. 6015

Wils, P., Ayiomamitis, A., Vanleenhove, M., et al. 2013, Photometry of High-Amplitude Delta Scuti Stars in 2012, IBVS, no. 6049

Wils, P., Ayiomamitis, A., Robertson, C. W., et al. 2014, Photometry of High-Amplitude Delta Scuti Stars in 2013, IBVS, no. 6122

Wils, P., Hambsch, F.-J., Vanleenhove, M., et al. 2015, Photometry of High-Amplitude Delta Scuti Stars in 2014, IBVS, no. 6150